INCREASING FRAME RATE OF LIMITED DIFRACTION IMAGING SYSTEM WITH CODE EXCITATIONS

Jian-yu Lu, Jing Wang, Hu Peng, and Jiqi Cheng[*]

1. ABSTRACT

Code excitations have been applied to the newly developed two-way dynamic focusing imaging method using limited diffraction array beams. Image frame rate is increased several folds. Computer simulations with both point scatterers and objects consisting of random scatterers were performed to demonstrate the efficacy of the method.

2. INTRODUCTION

Limited diffraction beams were first discovered by Stratton in 1941[1]. The most interesting feature of limited diffraction beams is that these beams, theoretically, can propagate to an infinite distance without changing their transverse beam patterns under the conditions that they are produced with an infinite aperture and energy. Even with a finite aperture and energy, they have a large depth of field. Because of this property, they can be applied to many fields such as medical imaging, tissue property identification, blood flow velocity vector measurement, nondestructive evaluation of materials, communications and other areas.

With limited diffraction beams, a high frame rate imaging method has been developed[2,3]. In this method, a single pulsed plane wave is used in transmission, and limited diffraction array beams are applied to received signals simultaneously. Three-dimensional images are constructed with a 3D inverse Fourier transform of the received data. Although this method produces a high image frame rate, the image resolution is

[*] Jian-yu Lu, Jing Wang, Hu Peng, and Jiqi Cheng are in the Ultrasound Laboratory, Department of Bioengineering, The University of Toledo, Toledo, Ohio 43606, U.S.A. Email: jilu@eng.utoledo.edu

lowered because the transmission beam is not focused. In addition, the image area is limited by where the transmission beam can illuminate.

Based on the high frame rate method and the reciprocal principle, limited diffraction array beams are also applied in transmission to construct images that are dynamically focused in both transmission and reception (a two-way dynamic focusing method)[4,2]. This produces an image of a very high quality in addition to a large field of view (over 90 degrees) and a higher signal-to-noise ratio (SNR)[4]. This method also achieves a similar image frame rate as conventional ultrasound B-scan imaging systems[5] where dynamic focusing is only performed in reception. If dynamic focusing were implemented in transmission also, the frame rate of a conventional system would be reduced by hundreds of folds. Although the two-way dynamic focusing method has several advantages, unfortunately, it is sensitive to motion artifacts because multiple transmissions are required and all echo signals are needed to construct a frame of image.

Code methods are widely used in many fields such as communication, radar and sonar system, and has been investigated by many reseachers[6,7]. This method has been extended recently to ultrasound imaging systems to increase the SNR and the effective ultrasound penetration into tissues[6,7]. In this paper, multiple codes with high autocorrelation and low cross-correlation are used to reduce the number of transmissions required to construct a frame of image in the two-way dynamic focusing method. In this method, up to three m-sequences[6,7] are transmitted simultaneously, each of which represent an array beam[8] of a different parameter (more codes can be used simultaneously to further reduce the number of transmissions for a frame of image if codes with higher autocorrelation and lower cross-correlation can be found). The received signals are separated with match filters. The outputs of the match filters produce signals that are used to replace those obtained from multiple transmissions of a single code or pulse. Because multiple codes are transmitted simultaneously, image frame rate are increased by a factor equal to the number of simultaneously transmitted codes and thus motion artifacts can be reduced.

To demonstrate the method, simulation of images of objects of a few point scatterers and multiple random point scatterers were carried out. Results show that although multiple code excitations increase the frame rate, contrast of constructed images are decreased due to higher range sidelobes as compared to that of short pulse excitations. To show the influence of range sidelobes of different codes on image quality, results of single frequency-modulated (FM) chirp excitations and single m-sequence excitations were also obtained. These results suggest that different codes exhibit different range sidelobes and thus a different image quality. Therefore, if codes of higher autocorrelations and lower cross-correlations can be found or designed, this method will be promising for medical ultrasonic imaging.

In the following, theories of two-way dynamic focusing imaging with limited diffraction array beams will be briefly introduced. Computer simulation results for code excitations will be presented, followed by a short discussion and conclusion.

3. THEORY OF TWO-WAY DYNAMIC FOCUSING IMAGING WITH LIMITED DIFFRACTION BEAMS

Constructions of images with the two-way dynamic focusing method are based on the following theory.

3.1. Limited Diffraction Array Beams

Limited diffraction array beams[8] are the important components of the two-way dynamic focusing method[4]. These beams can be obtained by multiplying X waves[9,10] with $i^n e^{-in\theta}$ and then summing the results over the index, n. For details, please see references[2,3,4].

$$\Phi_{Array}(\vec{r},t) = \sum_{n=-\infty}^{\infty} i^n e^{-in\theta} \Phi_{X_n}(\vec{r},t) = \frac{1}{2\pi} \int_{-\infty}^{\infty} T(k)H(k)e^{ik_x x+ik_y y+ik_z z} e^{-i\omega t} dk \quad (1)$$

where $0 < \theta < 2\pi$ is a free parameter, the subscript "Array" represents "array beams", $\vec{r} = (r,\phi,z)$ represents a spatial point in the cylindrical coordinates, t is time, r is radial distance, z is the axial distance, $k = \omega/c$ is the wave number, $\omega = 2\pi f$ is the angular frequency, f is the temporal frequency, c is the speed of sound or light, and X_n is the nth-order X wave.

$$(T(k)H(k)/c)e^{ik_x x+ik_y y+ik_z z} \quad (2)$$

is the Fourier transform (spectrum) of the array beams in terms of time,

$$H\left(\frac{\varpi}{c}\right) = \begin{cases} 1, & \omega \geq 0 \\ 0, & \omega < 0 \end{cases} \quad (3)$$

is the Heaviside step function[11], $T(k) = 2\pi B(k)e^{-ka_o}$, where $B(k)$ could be the transfer function of an imaging system, and

$$\begin{cases} k_x = k \sin\zeta \cos\theta = k_1 \cos\theta, \\ k_y = k \sin\zeta \sin\theta = k_1 \sin\theta, \\ k_z = k \cos\zeta = \sqrt{k^2 - k_1^2} \geq 0, \end{cases} \quad (4)$$

where

$$k_1 = \sqrt{k_x^2 + k_y^2} = k \sin\zeta \quad (5)$$

3.2. Two-way Dynamic Focusing Imaging

469

To construct 3D two-way dynamic focusing images, the same array transducer is used in both transmission and reception. In reception, the transducer is weighted to produce a limited diffraction array beam response with parameters of k_x and k_y. If a point scatterer is located at $\vec{r} = (x, y, z)$, the received echo signal is given by the following convolution (see (2))[2,4]:

$$R_{k_x, k_y, k}^{(one)}(t) = f(\vec{r})[\Phi_{ArrayT(\vec{r},t)} * \Phi_{ArrayR(\vec{r},t)}] = \frac{1}{2\pi} \int_{-\infty}^{\infty} \frac{T^2(k)H(k)}{c} f(\vec{r}) e^{ik_x x + ik_y y + ik_z z} e^{-i\omega t} dk, \quad (6)$$

where the subscript "ArrayR" means "array beam response in reception" and the response is the same as that in transmission, i.e., $\Phi_{ArrayR(\vec{r},t)} = \Phi_{ArrayT(\vec{r},t)}$, "*" represents the convolution with respect to time, $k_x = 2k_x$, $k_y = 2k_y$, $k_z = 2k_z$, the superscript "(one)" means "one point scatterer", and $f(\vec{r})$ is an object function (reflection coefficient) of a 3D object composed of randomly positioned point scatterers embedded in a uniform background supporting a constant speed of sound, c. Assuming the imaging system is linear, from (6) we obtain the echo signal from multiple scatterers[2,4]:

$$R_{k_x, k_y, k}(t) = \frac{1}{2\pi} \int_{-\infty}^{\infty} \frac{T^2(k)H(k)}{c} F(k_x, k_y, k_z) e^{-i\omega t} dk, \quad (7)$$

where $F(k_x, k_y, k_z)$ is the spatial Fourier transform of the object function.

From (7), a relationship between the temporal and spatial Fourier transforms are obtained:

$$F_{BL}(k_x, k_y, k_z) = c^2 H(k) R_{k_x, k_y, k}(\omega), \quad (8)$$

where $H(k)$ is used to indicate that only positive values of k are used and it can be applied to either side of the equation. It is clear from (8) that multiple array beams transmissions are required to construct a frame of image.

If the object function is independent of y, (8) can be simplified and used to construct 2D images. See References 2 and 4 for details.

4. CODE EXCITATIONS TO INCREASE IMAGE FRAME RATE

The temporal spectrum of the array beam in (1), $T(k) = 2\pi B(k) e^{-ka_0}$, is arbitrary. It can be the spectrum of a short pulse, an FM chirp, or an m-sequence.

To increase frame rate of the two-way dynamic focusing method given by (8), multiple codes need to be selected and transmitted simultaneously. Each code is associated with a limited diffraction array beam of different parameters. Received echo signals are processed with match filters to separate signals from different array beams. After signals are separated, images can be constructed with (8)[2,4]. If N codes are selected, the image frame rate can be increased by N times. Ideally, codes whose autocorrelations

470

are a δ-function with no cross-correlations should be used. However, in practice, the ideal conditions are not achievable resulting in high range sidelobes and reduced image contrast.

Many codes have been investigated in the literature[6,7]. The autocorrelation of Golay code pairs is a δ-function with zero cross-correlation. However, about the same number of transmissions is required if Golay codes are to be used to construct images in the two-way dynamic focusing method. Therefore, the Golay codes are not suitable for our application. The same problem is with the Hadamard codes. A pseudo FM chirp may have a low range sidelobe, especially, when it is weighted with a smooth window function. However, multiple pseudo FM chirps having the same spectral band have high cross-correlations and thus are difficulty to separate after they are transmitted simultaneously. If their spectral bands are different, they are not suitable for biological soft tissues because of the frequency-dependent attenuation of the tissues. For the reasons above, in this paper, only multiple m-sequences are studied to increase image frame rate.

5. COMPUTER SIMULATION AND RESULTS

In the computer simulation, 3 m-sequences of a length of 127 chips and 25.6 μs time duration were used. They were chosen from 9 m-sequences that were obtained from 7-bit linear feedback shift-registers[6,7]. The lowest cross-correlation of the m-sequences we selected are about 13% of the autocorrelation peak due to the finite length of the code sequences.

The geometry of the transducer for the simulation is based on a 64-element linear array used in the experiment of Reference 3. In the simulation, the center frequency of about 2.5 MHz is assumed, and the one-way bandwidth of the array is about 81% of the center frequency. Because the system is 2D with a linear array, the parameter, k_y, of the array beam in (1) is set to 0. In this case, the elevation thickness of the array is irrelevant.

Two image phantoms are used in the simulation. The first consists of 9 point scatters (can be viewed as line scatterers in 2D case) and their locations are given in Fig. 1 of Reference 4. The other phantom consists of 5 cylindrical scattering objects embedded in a uniform scattering background. The overall dimension of the image is the same as that of the first phantom (see Fig. 1 of Reference 4). There is in average 1 scatterer in each λ^2 of the second phantom and scatterers are randomly distributed, where λ is the center wavelength. Assuming the speed of sound is $1.5mm/\mu s$ in the medium, the wavelength is about 0.6 mm and thus the total number of scatterers is about 7919. The 5 cylindrical scattering objects in the second phantom have the following parameters: object #1, 2, 3, 4, and 5 have a diameter of 15 mm, 15 mm, 15 mm, 6 mm, and 6 mm, respectively, and their reflectivity contrasts relative to the background in dB scale are +15dB, $-\infty$ dB, -15dB, +15dB, and -15dB. The centers of these objects are shown in the constructed image in the following.

Images of the phantoms of the 9-point scatters and 7919 random scatterers were constructed with the two-way dynamic focusing method in (8) and are shown in Figs. 1 and 2, respectively. Because a cosine function aperture weighting was applied to both transmission and reception on the linear array (the weighting has a peak at the center and

zero at the edges of the array), the constructed images are darker (about 15 dB lower in brightness) on the edges. To compensate, an inverted modified Hamming window function (Fig. 3) was multiplied with the constructed images in the transverse direction:

$$B(x) = 1/(0.19 + 0.81\cos^2(\pi(x - (X/2))/X)) \tag{9}$$

where $0 < x \le X$ is the transverse coordinate and X is the width of the constructed images (76.8 mm) (The original Hamming window is given by: $1.0 - 0.92\cos^2(\pi x/X)$).

For comparison, images with a short pulse ($0.6\,\mu s$ length), a pseudo FM chirp (2.5 MHz bandwidth and $25.6\,\mu s$ length, weighted with a Hamming window modified by a power of 0.66), and a single m-sequence ($25.6\,\mu s$ length) were also constructed (see panel (a), (b), and (c) in both Figs. 1 and 2).
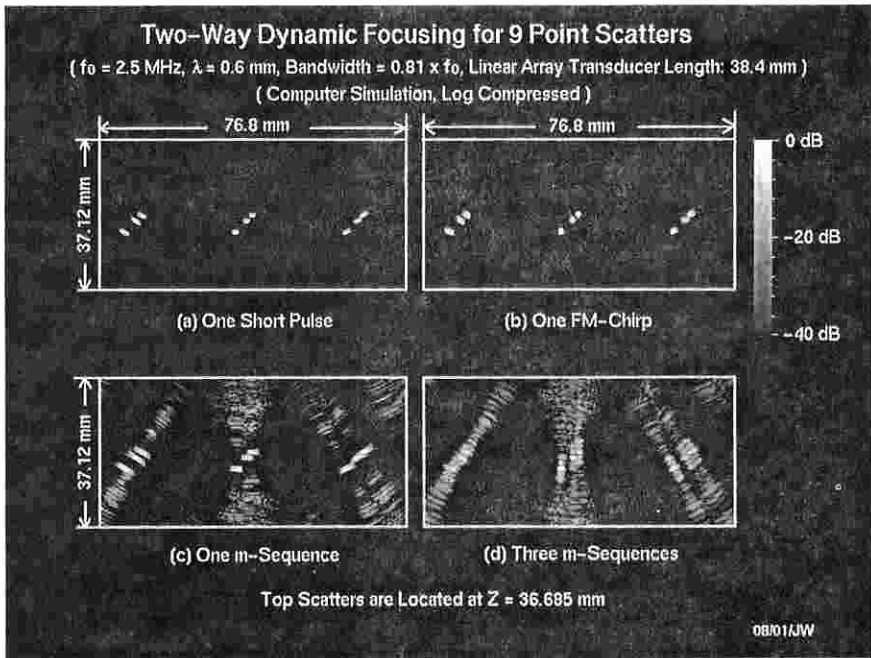

Fig. 1. Image of 9 point scatters constructed with the two-way dynamic focusing method. Images in all panels are 40dB compressed. A cosine aperture apodization was applied in the construction. An inverted modified Hamming window function was multiplied with all panels in transverse direction of constructed images. Four different excitations were used for comparison: (a) one short pulse, (b) one FM chirp, (c) one m-sequence, and (d) three m-sequences.

ƒ
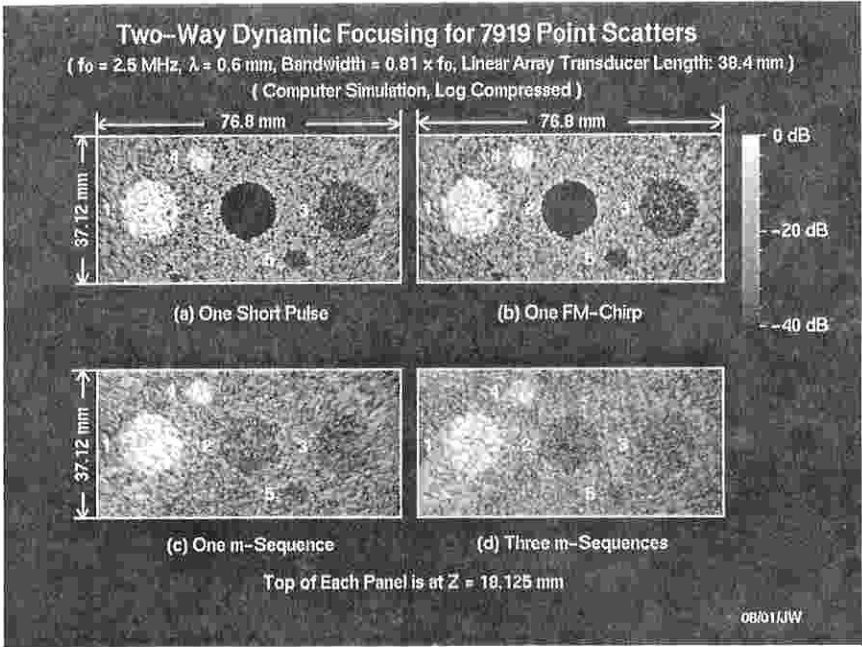
Fig. 2. This figure has the same layout and was constructed under the same conditions as those of Fig. 1, except that 5 scattering objects (see the numbers in the images) and a total of 7919 random scatters are used in the image construction.
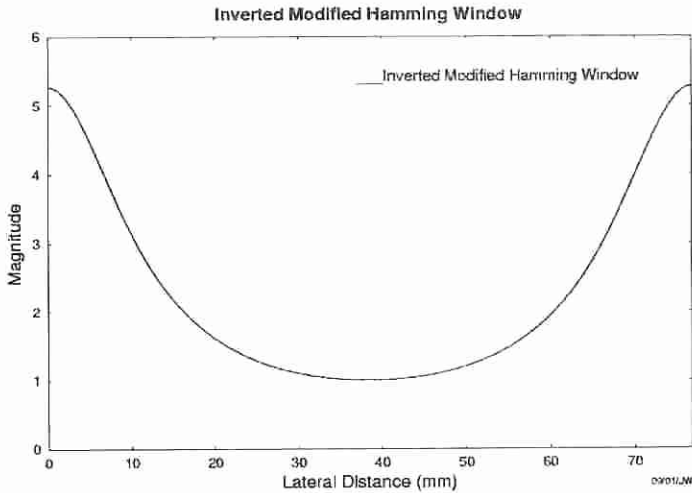
Fig.3. Inverted modified Hamming window function for brightness compensation of Figs. 1 and 2.

473

6. DISCUSSION

From Figs. 1 and 2, it is seen that image contrast are reduced when range sidelobes increase. With 3 m-sequences, although the image frame rate is increased by 3 folds, image constrast is lowered as compared to either short pulse or FM chirp excitation. Even with a single m-sequence, the contrasts of constructed images are also lower due to its higher range sidelobes of autocorrelation. Table 1 gives a list of contrasts of the objects relative to the background of images in Fig. 2 for different excitations.

Table 1. Contrasts of Constructed Images

CONTRAST (dB)	Object 1	Object 2	Object 3	Object 4	Object 5	Background
Ideal	15	-∞	-15	15	-15	0
1 Short Pulse	14.69	-28.12	-13.40	14.93	-14.15	0
1 FM Chirp	14.63	-24.93	-14.40	14.74	-13.44	0
1 m-Sequence	14.31	-5.66	-7.10	14.45	-7.56	0
3 m-Sequences	14.37	-4.05	-5.04	14.10	-4.58	0

From the property of m-sequences, the lowest cross-correlations of 127-chip m-sequences are about 13% or -17dB. When several m-sequences are used, the cross-correlations will be higher leading to high range sidelobes. To reduce range sidelobes and cross-correlations, longer sequences are preferred. However, a longer sequence will increase the blank range of constructed images near the transducer because echo signals can only be received after the transmission process is completed. For example, if the code length is 127, with a center frequency of transducer of 2.5 MHz and assuming one period contains 2 chips, the depth of blank image is about 19.2 mm. If a code with 1023 chips is used (corresponding to the lowest cross-correlation of about 3% or -30dB), the blank depth of images will be 153.6 mm, which is unacceptable for most of the applications. Therefore, there is a trade-off between the image blank depth and the length of m-sequences.

If codes with low cross-correlation and high auto-correlation can be found, image frame rate of the two-way dynamic focusing method can be increased while maintaining a high image contrast.

7. CONCLUSION

Code excitations have been applied to the newly developed two-way dynamic focusing imaging method[2,4]. This increases the image frame rate by several folds at the expense of a lower image contrast due to increased range sidelobes. Range sidelobes can be reduced if a longer code is used. However, this increases the blank depth of constructed images because echoes can only be received after the transmission process is completed. If codes of a high autocorrelation and low cross-correlation can be found,

image frame rate of the two-way dynamic focusing method can be further increased without compromising the image contrast. This will be a topic of our future research.

8. ACKNOWLEDGEMENT

9. REFERENCES

1. J. A. Stratton, Electromagnetic Theory. New York and London: McGraw-Hill Book Company, 1941, Page 356.
2. Jian-yu Lu, "2D and 3D high frame rate imaging with limited diffraction beams," IEEE Transactions on Ultrasonics, Ferroelectrics, and Frequency Control, vol. 44, no. 4, pp. 839–856, July, 1997.
3. Jian-yu Lu, "Experimental study of high frame rate imaging with limited diffraction beams," IEEE Transactions on Ultrasonics, Ferroelectrics, and Frequency Control, vol. 45, no. 1, pp. 84--97, January, 1998.
4. Jian-yu Lu, "Transmit-receive dynamic focusing with limited diffraction beams," in IEEE 1997 Ultrasonics Symposium Proceedings, 97CH36118, vol. 2, pp. 1543-1546, 1997. (ISSN: 1051-0117)
5. F. S. Foster, J. D. Larson, M. K. Mason, T. S. Shoup, G. Nelson, and H. Yoshida, "Development of a 12 elemnet annular array transducer for realtime ultrasound imaging," Ultrason. Med. Biol., vol. 15, no. 7, pp. 649-659, 1989.
6. Matthew O'Donnell, "Coded excitation system for improving the penetration of real-time phased-array imaging systems", in IEEE Transactions on Ultrasonics, Ferroelectrics, and Frequency Control, vol. 39, no. 3, pp. 341-351, May, 1992.
7. Richard Y. Chiao, Lewis J. Tomas, and Seth D. Silverstein, "Sparse array imaging with spatially-encoded transmits", in IEEE 1997 Ultrasonics Symposium Proceedings, pp. 1679--1682, 1997.
8. Jian-yu Lu, "Limited diffraction array beams," International Journal of Imaging System and Technology, vol. 8, no. 1, pp. 126-136, January, 1997. (ISSN: 0899-9457)
9. Jian-yu Lu and J. F. Greenleaf, "Nondiffracting X waves --- exact solutions to free-space scalar wave equation and their finite aperture realizations," IEEE Transactions on Ultrasonics, Ferroelectrics, and Frequency Control, vol. 39, no. 1, pp. 19--31, January, 1992.
10. Jian-yu Lu and J. F. Greenleaf, "Experimental verification of nondiffracting X waves," IEEE Transactions on Ultrasonics, Ferroelectrics, and Frequency Control, vol. 39, no. 3, pp. 441--446, May, 1992.
11. R. Bracewell, The Fourier Transform and its Applications. New York, NY: McGraw-Hill Book Company, 1965, chs. 4 and 6.